INTERNATIONAL JOURNAL OF INNOVATIVE RESEARCH & DEVELOPMENT

ISSN: 2278 – 0211 (Online) / 2278-7631 (Print)

A Compact and Versatile UHV Chamber for High Resolution Spectroscopy Using Laser Excited Atomic Fluorescence Spectroscopy (LEAFS)

GudimellaVenkataSatagopAcharyulu,
MandaSankari,
PragadaVelanganiKirankumar
and
MandaVenkataSuryanarayana
National Centre for Compositional Characterisation of Materials
Bhabha Atomic Research Centre,
Hyderabad, India

Abstract: *Aresistively heated graphite tube atomic beam apparatus and a compact laser-atom interaction chamber for sub-Doppler fluorescence experiments have been developed.We have studied the evolution of the system from Doppler broadened conditions to Doppler limited conditions which enabled us to study the sub-Doppler hyperfine spectroscopy of rubidium and potassium. The compact interaction geometry, flexibility in changing the atomic beam source and simplicity of the entire set up make it useful for the measurement of isotope shifts and hyperfine structure measurement of single / multistep excitations of various elements.Test experiments were conducted with the atomizer by loading rubidium and potassium in order to find the optimum design conditions for the set-up. The sub-Doppler hyperfine structure peaks of the* ^{85}Rb *and* ^{87}Rb *isotopes have been measured and the full width at half maximum of the recorded peaks are ~16 MHz for the* $5^2S_{1/2} - 5^2P_{3/2}D2$ *transition of rubidium which is close to the natural broadening of this transition.The total number of rubidium atoms leaving the source aperture is estimated to be 2.7* $\times 10^{14}$ *atoms / sec.The number of rubidium atoms in the region of interaction is 2.4* $\times 10^{9}$ *atoms /* cm^2 *in a laser beam of 0.3cm diameter. The sub-Doppler hyperfine structure of the* ^{39}K *and* ^{41}K *isotopes has also been recorded for the* $4^2S_{1/2} - 5^2P_{1/2}$ *D1 transition of potassium. The overall detection efficiency of the LEAFS process is found to be ~2 x* 10^{-11}.

Keywords: *Isotope shift, hyperfine structure, atomic beam source, fluorescence detection, Doppler free spectroscopy*

PACS:

31.30.Gs **Hyperfine interactions and isotope effects** *(see also 32.10.Fn Fine and hyperfine structure)*

2.50.+d **Fluorescence, phosphorescence (including quenching)**

07.30.Kf **Vacuum chambers, auxiliary apparatus, and materials**

07.77.Gx **Atomic and molecular beam sources and detectors (see also 37.20.+j Atomic and molecular beam sources and techniques, in atomic and molecular physics)**

Introduction

Several research groups have carried out atomic fluorescence experiments on a wide ranging combination of atomization sources/dispensers or MOTs for various applications [1 – 11].An accurate knowledge of fundamental atomic quantities is useful not only for atomic physics experiments but also for fields like astrophysics, plasma physics and fusion physics. Altaf et.al [12]have used the resonance fluorescence spot technique to measure transition frequencies and isotope shifts with an accuracy of 60 MHz for ytterbium isotopes. Prompt fluorescence from metastable states of ions has also been studied to determine lifetimes of metastable states [13]. Fluorescence of a highly collimated cesium atomic beam has been reported by Gerginov and Tanner [14]. Time resolved laser induced fluorescence has also been used for lifetime measurements in lanthanumions [15]. We have constructed this compact UHV chamber for frequency locking of lasers and for carrying out spectroscopic measurements.

In our system the laser induced fluorescence chamber consists of three sub systems. The source chamber houses the resistively heated graphite tubeatomizer.The atomic beam of rubidium is produced by electro-thermal evaporation from a heated sample of a mixture of rubidium chloride and potassium nitrateplaced in a graphite crucible.The atomizer is closely coupled to the interaction region. The graphite crucible has two advantages as an atomization source. The first advantage being, most of the methodology developed over several decades in flameless atomic absorption spectroscopy (FAAS)can be put to use for the generation of neutral atomic species [16]. Secondly the long channel of the graphite crucible helps in self collimation. The atoms effuse out of the source chamber through a small aperture (ϕ = 2 mm) into a port which hasa collimator and enter the laser interaction chamber where the atomic beam is intersected orthogonally by the laser beam. The chamber has two pumping ports to efficiently pump the atomic cloud that is outside the divergence limit of the collimators and any other residual gases present in the chamber.

Experimental system

The preparation of free atoms in atomic beams is necessary to study their properties and here it comprises of atom-photon interaction.The laser induced fluorescence from the atomic system is monitored.The choice of the right crucible

material is crucial for the successful operation of a metal atom beam source. The high density graphite used as crucible material has low outgassing rates at elevated temperatures and the heat transfer to the environment is a minimum.The long canal of the graphite crucible functions as a self-collimating atomic beam source to provide more efficient transport of atoms into the laser – atom interaction region. The directionality of the atomic beam has been achieved by the combination of the oven aperture and operating in a regime where the Knudsen number (K_n), the ratio of the mean free path of the source atoms to the diameter of the aperture of the oven, is greater than unity. The sample which is a mixture of rubidium chloride and potassium nitrate was loaded into a graphite crucible. The crucible is machined from high purity graphite with dimensions of ϕ = 2 mm for the inner diameter, a wall thickness of 1mm and a depth of 27 mm.The crucible is held by two graphite cups. The entire atomizer is mounted on to one of the side ports of the chamber.A DC power supply (120 Amp, 20 Volts) was used for heating the graphite crucible. The power supply was operated in a constant current mode. The crucible is mounted between two water cooled electrodes and graphite cups at the contact points to centre the crucible and allow higher temperature operation. The entire crucible assembly is mounted on a CF-100 flange with water cooling channels and high current feed throughs. This assembly is mounted in a differentially pumped forechamber which allows rapid changing of samples and minimum down time. The graphite crucible facilitates carbothermic reduction in the mixture which enables the release of the rubidium atomic vapour. The compact size of the source makes the turn-on and the turn –off times relatively less in comparison to thehours of operation of the atomic beam. The turnaround time is typically about 2 hours.

An UHV chamber has been designed, fabricated and vacuum tested for detecting atomic beam fluorescence from a collimated atomic beam source. The experimental chamber has a cuboidal shape with six ports on the six faces of a cube. One of the ports houses the arm that has the source chamber containing the atomic beam furnace. The schematic of the entire LEAFS set-up is shown in figure 1.

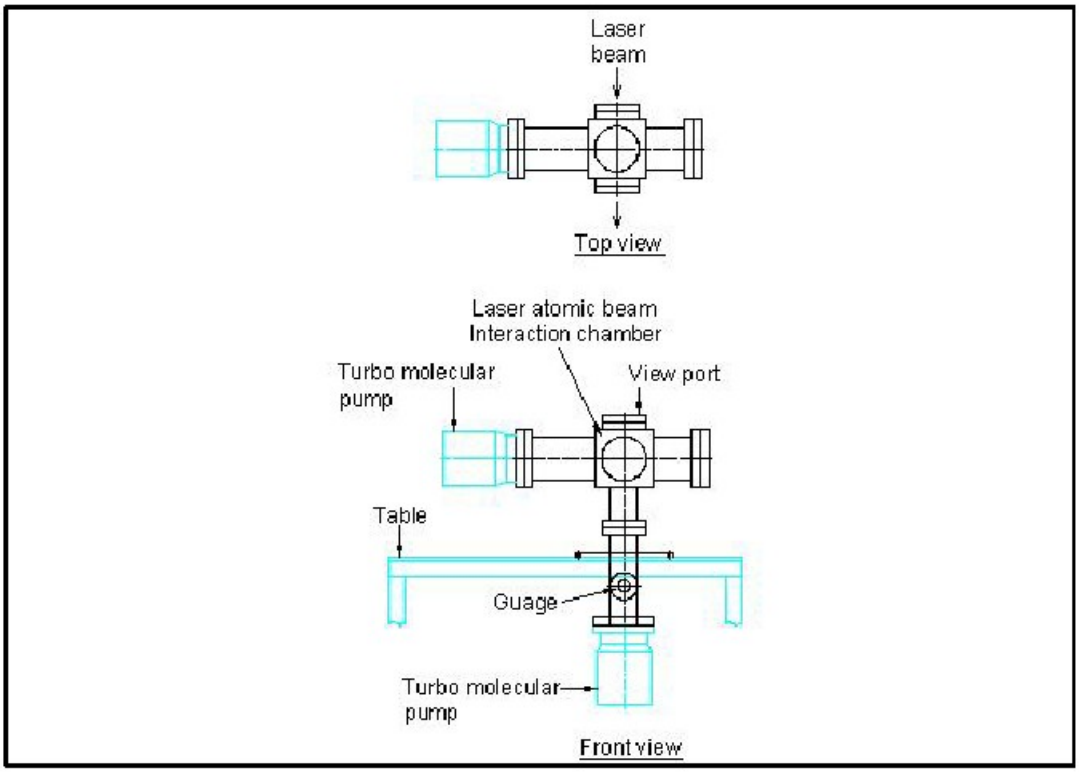

Fig. 1: The schematic of the UHV chamber showing the top view and the front view of the set-up.

The temperature of the atomizer has been measured with a two colour optical pyrometer. Three of the portshave CF-100 flanges and one of the ports houses the arm that is attached to a pumping station.The clear optical view of the three ports is (ϕ) 50 mm. Light resonant with the $5^2S_{1/2}$– $5^2P_{3/2}$rubidium D2 transition was generated by a cw- ring Ti: Sapphire laser pumped by a 10 W DPSS laser. The experimental set-up is depicted in figure 2.

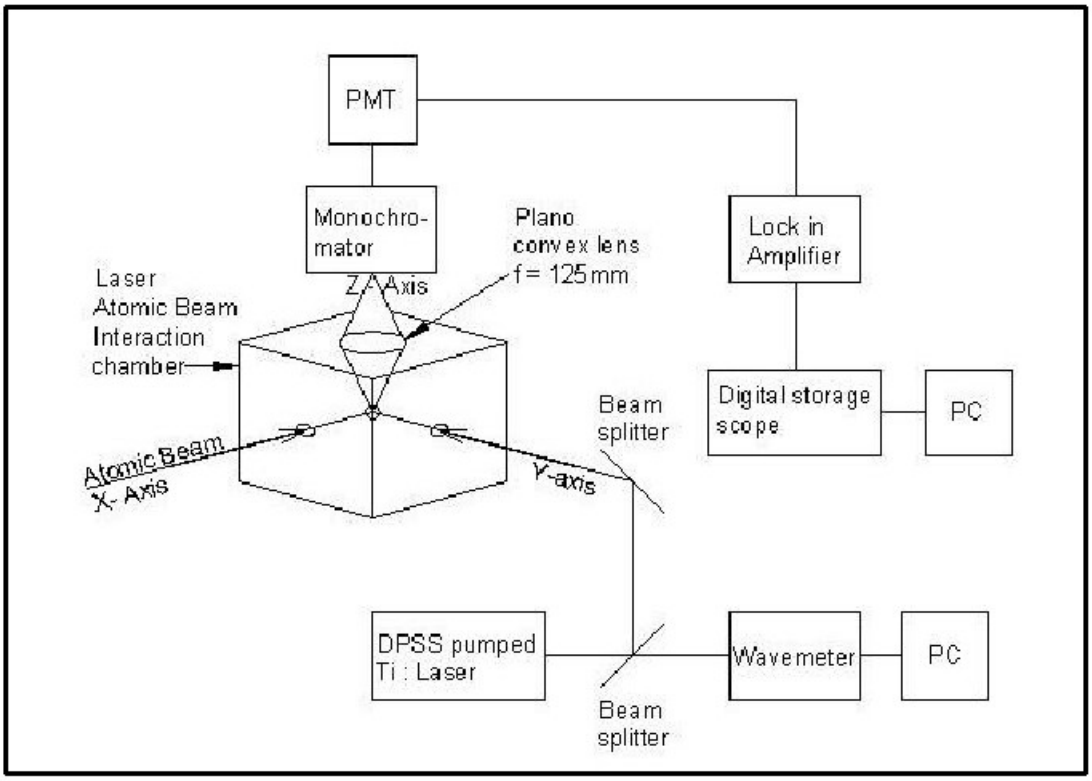

Fig. 2 : Schematic of the experimental set-up in LEAFS with the laser-atomic beam interaction in the xy plane and detection of the fluorescence photons in the z-plane.

To establish differential pumping, two turbo molecular pumping stations of capacity 250litres/sec are used. The other pumping station is opposite to the source side. The vacuum at the source side is ~2 x 10^{-6} mbar and the vacuum at the interaction chamber is 2 x 10^{-7} mbar. The source chamber and the interaction chamber are connected by a long tube which forms one of the six ports of the cuboidal chamber. This tube houses a 75 mm long SS collimator block with a6mm diameter hole in the centre. This SS block has been designed with sufficient number of 4 mm holes on the circumference to pump away the divergent atomic beam and any residual gases present in the chamber. The novelty is that the specific design of the SS collimator block has enabled in establishing differential pumping between the source and the interaction chamber. The holes in the periphery of the collimator are placed in staggered configuration to prevent the scattered laser light and other stray radiation from atomizer reaching the interaction region. This arrangement minimizes the thermal electrons, ions and black body radiation originating from the beam source reaching the photo multiplier tube and thus suppressing the background.

The cold surfaces of the intermediate arm, and the SS collimation block serve as cold adsorption pumps for the divergent rubidium vapor exiting the source. Only rubidium atoms streaming straight through the aperture holes are able to reach the experimental chamber without striking a surface. The cold pumping is a key feature of which is responsible for the differential pumping in our system. The emitted resonance fluorescence is focused onto a Czerny Turner monochromatorusing a f= 125 mm plano convex lens. This monochromatorenables reduction of stray light and thus the S/N ratio of the fluorescence signal significantly improved. The fluorescence signal was then detected by a photomultiplier tube. The novelty in the design has allowed us to take the raw signal from the PMT and hence the simplicity in the detection of the signal. There is no electronics associated with the signal processing. There is no electronics associated with the signal processing (no signal amplification, no lock in amplification etc). This raw signal has allowed us to work in the nanogram range. A 1000 time signal amplification will straight lead to detection limit in the picogram range using the present system.

For some of the experiments when the signal was very weak (~ 5 mV) it was amplified using a lock in amplifier.The hyperfine spectrum was recordedusing a digital storage oscilloscope. The dimension of the fluorescence imageis found to be ~ 3mm x 6mm.The fluorescence from the ^{85}Rb atom has been imaged through the view port (Fig.3).

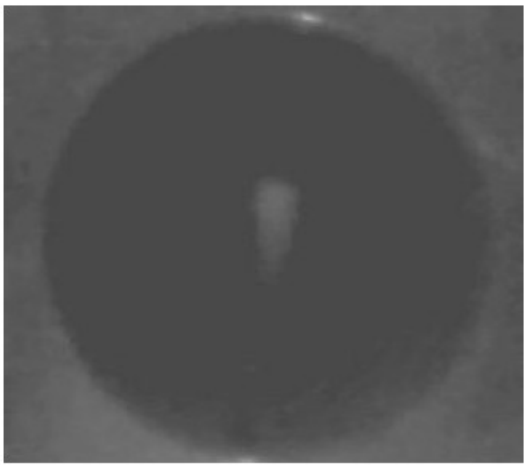

Fig. 3:The web camera image of the ^{85}Rb fluorescence.

This imaging of the atomic fluorescence allowed to verify the existence of the atomic beam and also to align the probe laser and the detected fluorescence. A small fraction of the light is fed to awavemeterwith a resolution of 30 MHz to monitor the laser wavelength.

Results and discussion

In order to characterize the rubidium atomic beam,laser excited atomic resonance fluorescence has been performed on the $5S_{1/2} - 5P_{3/2}$D2rubidium transitions. The probe laser wavelength is 384.229295 THzwhich is produced using a DPSS pumped Ti:Sa laser.Initially we observed Doppler broadened fluorescence peaks of the ^{85}Rb and ^{87}Rb isotopes with a full width at half maximum (FWHM) of 450 MHz (Fig.4).

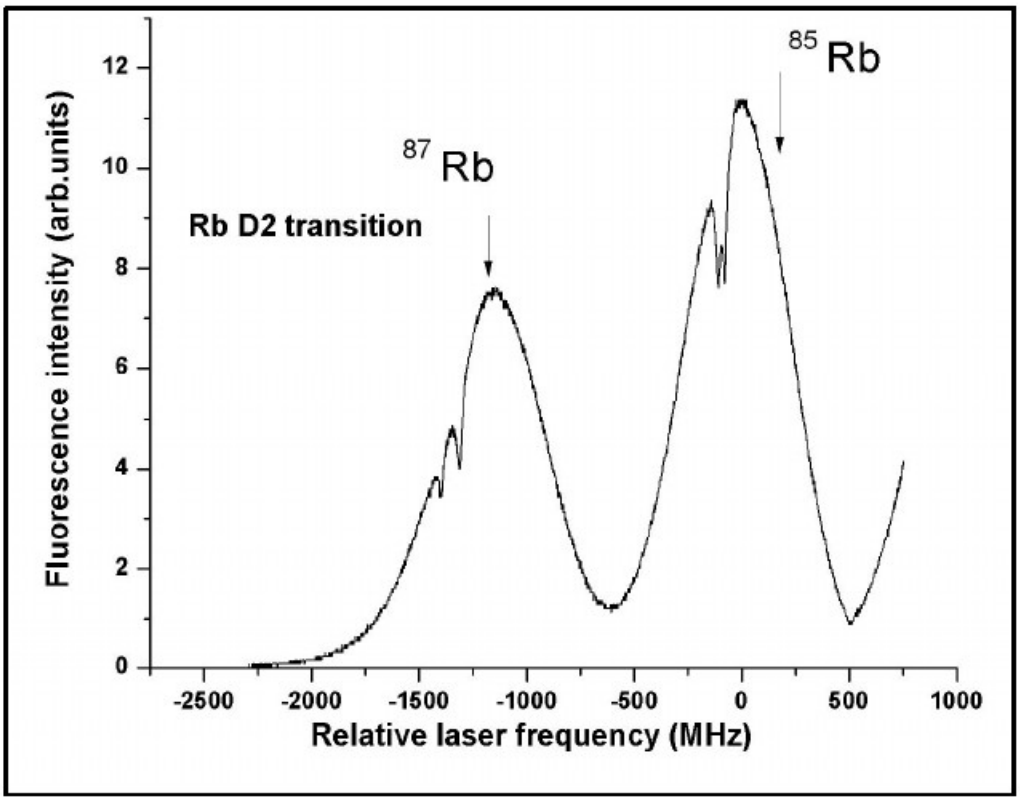

Fig. 4: The Doppler broadened peaks of the ^{85}Rb and the ^{87}Rb isotopes of the $5S_{1/2}$ - $5P_{3/2}$ D2 transition. The dips in the fluorescence peaks are due to cross over resonances

This indicates that atomic beam conditions were still not prevailing at the laser-atom interaction region. The Doppler broadening $\delta\nu_D$ is given by the expression

$$\delta\nu_D = 7.16 \times 10^{-7}\left[\sqrt{T/M}\right]\nu_o \qquad (1)$$

Where, T is the temperature of the source in K, M is the mass of rubidium in a.m. u and ν_o is the frequency (384.229295 x 10^{12} Hz) of the transition in Hz.At a source

temperature of 950 K the Doppler width is 910 MHz. The residual Doppler width $\delta\nu_{rdw}$ is given by the expression

$$\delta\nu_{rdw} = 7.16 \times 10^{-7} \left[\sqrt{T/M} \right] \nu_o \, Sin(\theta) \qquad (2)$$

Where θ is the angle of divergence of theatomic beam.In the absence of collimation, the angular divergence of the rubidium cloud was 14.3^0. The residual Doppler width $\delta\nu_{rdw}$ is ~225MHz. Therefore the FWHM of the peak in figure 5 is twice the $\delta\nu_{rdw}$ which, corresponds to 450 MHz.After analysis of the UHV chamber and the design of the atomic beam furnace, we found that, a collimated atomic beam is not formed at the interaction region due to improper collimation and poor vacuum at the laser-atom interaction region. The laser beam reflected from one of the view ports, acts as a probe beam and hence the cross over resonances are observed as dips in the Doppler broadened pedestal as also observed in the case of saturation absorption spectroscopy(Fig.5). But the Doppler narrowed atomic beam fluorescence signal is seen emerging over the large Doppler broadened atomic resonance(Fig.5).An additional collimator has been designed and positioned after the atomizer to narrow the Doppler peaks.

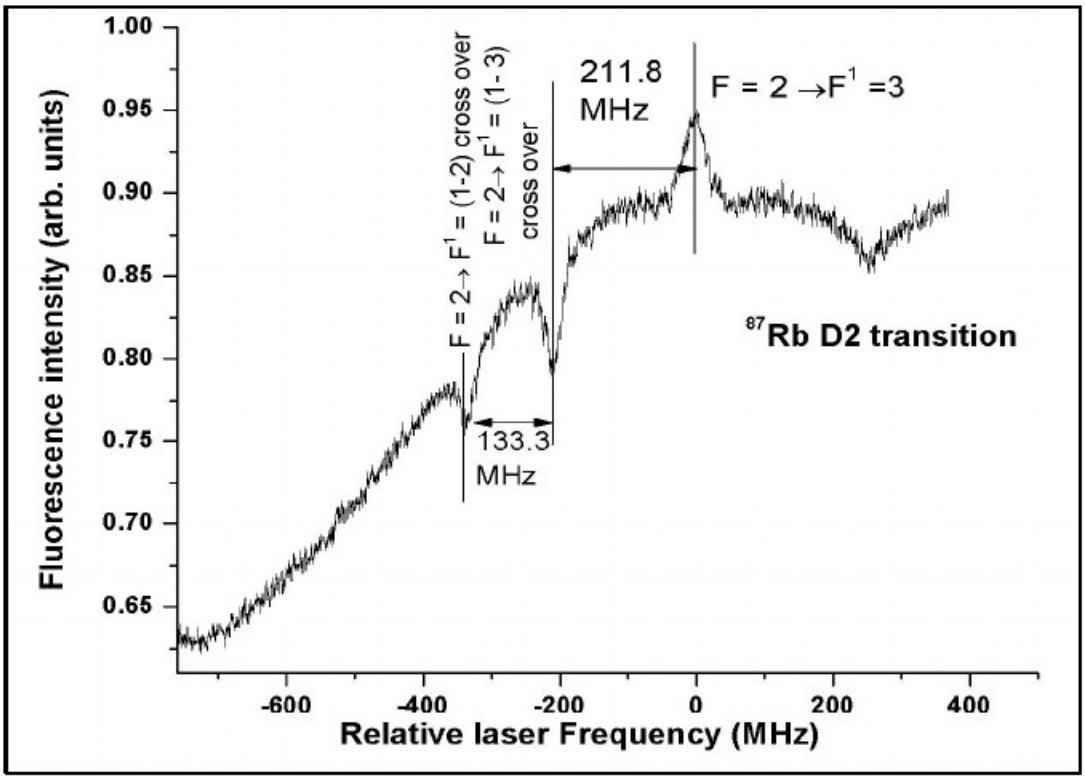

Fig.5: The sub-Doppler resonances are observed to be riding over the Doppler broadened pedestal. The signal due to the F = 2 to F^1 = 3 is also seen emerging

Doppler broadening limits the resolution of optical spectroscopy.The crossed-beam method is a simple way to reduce the Doppler broadening on a transition. The laser beam intersects the atomic beam close to right angles. A slit collimates the atomic beam to give a small angular spread [17]. Experiments have been performed at various distances from the exit orifice of the crucible with the introduction of slits and collimator in order to have varyingcollimation ratiosand Doppler broadening conditions.This helped us in making various modificationsto the chamber like the introduction of additional vacuum pump and differential pumping.

Initiation of atomic beam conditions and suppression of Doppler broadened background is observed in figure 6. In figure 6, the signal which is due to the atomic beam is collision free and is seen to be riding over the Doppler pedestal. The vacuum in the chamber is not conducive for carrying out sub-Doppler experiments. Turbulent flow was causing collisions in the atomic beam and hence, Doppler pedestal still exists. An additional pump near the interaction chamber was added to create differential pumping and to improve the vacuum at the laser-atom interaction region.

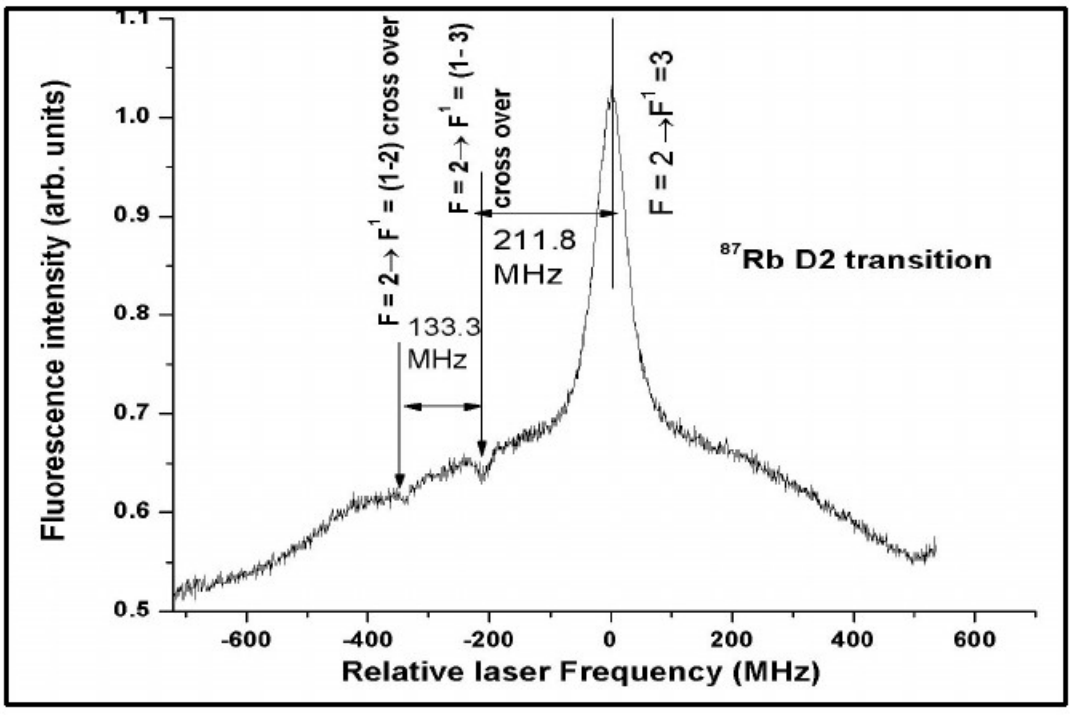

Fig.6:The initiation of atomic beam conditions, the emergence of a narrow signal and the suppression of Doppler background

The fluorescence spectrum is recorded by inclusion of a collimator, an additional joint to the UHV chamber. The chamber was slightly redesigned with a provision for differential pumping. With this modification, the Doppler width could be reduced for the rubidium D2 transition.The intensities of the various hyperfine components correspond to the expression for relative intensities of single photon electric dipole allowed transitions in IJ coupling and thereby indicating partial presence of optical pumping effects and therefore marginal change in the relative intensities.

Atomic beam fluorescence spectrum for the entire spectral range of the ^{87}Rb and the ^{85}Rbisotopes have been recorded after improving the vacuum conditions by including an additional turbo molecular pump. Thus reducing the collisional broadening the width could be further reduced and the sub-Doppler peaks of both the isotopes have been recorded (Fig. 7). All the electric dipole allowed rubidium transitions from the ground $5S_{1/2}$ state to the excited $5P_{3/2}$ state for the ^{87}Rb isotope and the ^{85}Rb isotope could be clearly resolved and is shown in figure 7A along with the simulated spectrum figure 7B. The order of the components is written in the order of increasing frequency.

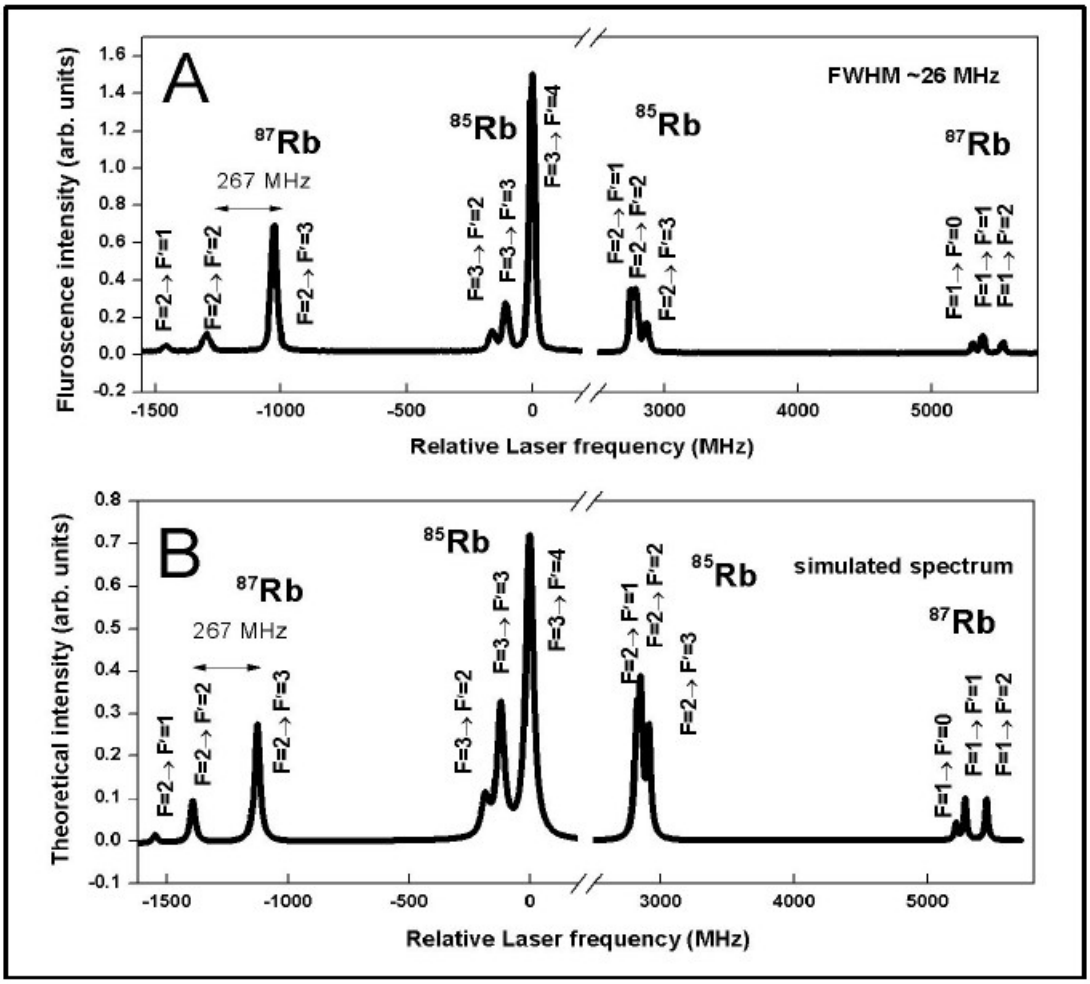

Fig. 7:Experimental (A) as well as the theoretical (B) laser induced fluorescence spectrum for the $5S_{1/2} - 5P_{3/2}$ D2 transition of rubidium spanning the entire range covering the hyperfine spectrum of ^{87}Rb and the ^{85}Rb isotopes.The sub-Doppler peaks of both the isotopes are seen whose FWHM is ~ 26 MHz

In the developed system, the spectral resolution is limited by the residual Doppler width. The best possible spectral width that we could get was FWHM ~ 16 MHz (Fig.8).Under these conditions the atomic flow was collision free and the sub Doppler peaks could be recorded. The major peak is for the F=2 to F^1=3 hyperfine transition and the smaller peak is the F=2 to F^1 = 2hyperfine transition (Fig.8). However, the less intense hyperfine transitions could be observed only as feeble signals just above the background. One could clearly observe the complete suppression of the Doppler broadened pedestal and the clean Doppler narrowed fluorescence peak clearly indicate

collision free atomic beam conditions at the laser-atom interaction region.Step by step modification clearly shows the evolution of the system from Doppler broadened conditions to Doppler limited conditions as seen from the figures (figure 4 through figure 8).

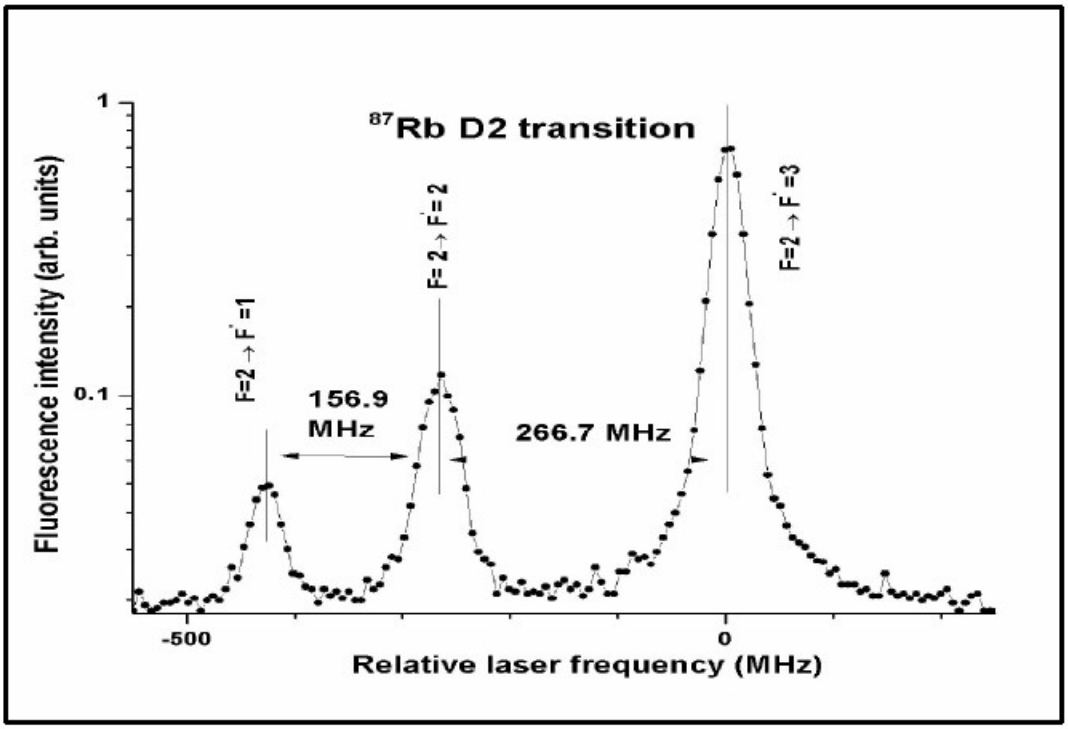

Fig.8:The sub-Doppler peaks for the ^{87}Rb isotope for the D2 transition have been recorded. The major peak is for the F=2 to F^1=3 hyperfine transition and the smaller peaksare the F=2 to F^1 = 2 transition and the F=2 to F^1 = 1transition. The FWHM of the transition is observed to be ~ 16 MHz

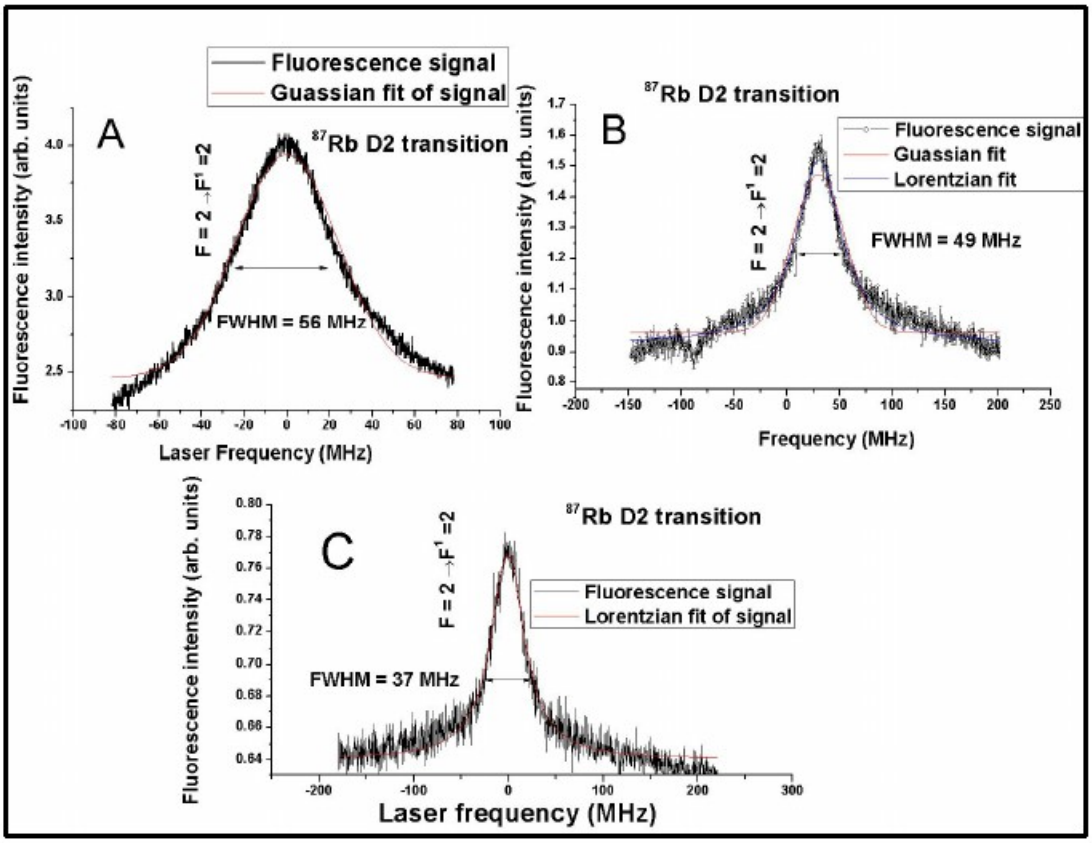

Fig. 9:The F = 2–F^1 = 2 hyperfine component of the D2 line of ^{87}Rb at various laser powers. A) Laser power of 19 mW and the scan width is 160 MHz. B) Laser power of 1.9 mW and the scan width is 350 MHz and C) Laser power of 100 μW and the scan width is 350 MHz

The fluorescence spectrum has been recorded for various power conditions. Fig.9a is for a laser power of 19 mWand the scan range was ~2.3 GHz, bias given to the PMT was -990V and the furnace was operated at a current of ~52 Amps. The ^{87}Rb hyperfine peak has been recorded and the scan width as observed in the wavemeteris 160 MHz.The FWHM of the peak is ~49 MHz.The power has been reduced ten times and the spectrum recorded. For a laser power of 1.9 mW, the scan width as observed in the wavemeter is 350 MHz.The narrow Doppler fluorescence peak for ^{87}Rb isotope for the hyperfine transition F=2 to F^1=2 is recorded (Fig.9b). The FWHM of the peak has been estimated to be ~48MHz. The laser power was further reduced to 100 □W power and scanrange as observed in the wavemeter is 350MHz. The narrow Doppler fluorescence peak for the F=2 to F^1 = 2 peak for ^{87}Rb has been recorded at lower power and the FWHM has been

estimated to be ~37 MHz (Fig.9c). By optimizing the various conditions like the laser power, the temperature of the atomic beam furnace, the focal length of the focusing lens and minimizing the stray light background to a large extent, the linewidth of the fluorescence peaks have been brought down to ~ 16 MHz (Fig.8).Thus the spectral width is approaching the natural width of the $5S_{1/2}$ - $5P_{3/2}$rubidium D2 linefor ^{87}Rb which is 6 MHz.Collimation reduces the Doppler broadening by a factor of sine of the angular divergence of the atomic beam. Hence a Doppler width of 910 MHz at a temperature of 950 K is reduced to 20 MHz after good collimation of the atomic beam. Only the velocity group which is in the very centre of the Maxwellian velocity distribution curve is selected and hence the angular divergence of the atomic beam is ~1^0. Therefore adjusting the throughput and the collimation of the atomic beam,the fluorescence spectrum has been recorded. For certain experiments the temperature was reduced and the atomizer was operatedat ~ 850K and the hyperfine spectrum of the ^{87}Rb isotope was recorded. The sub-Doppler peaks for the ^{85}Rb isotope for the D2 transition have been recorded. The order of the components in the order of increasing frequency is F=2 to F^1=3component, F=2 to F^1=2 component and then the F=2 to F^1=1 component. The components are very well resolved (Fig.10).

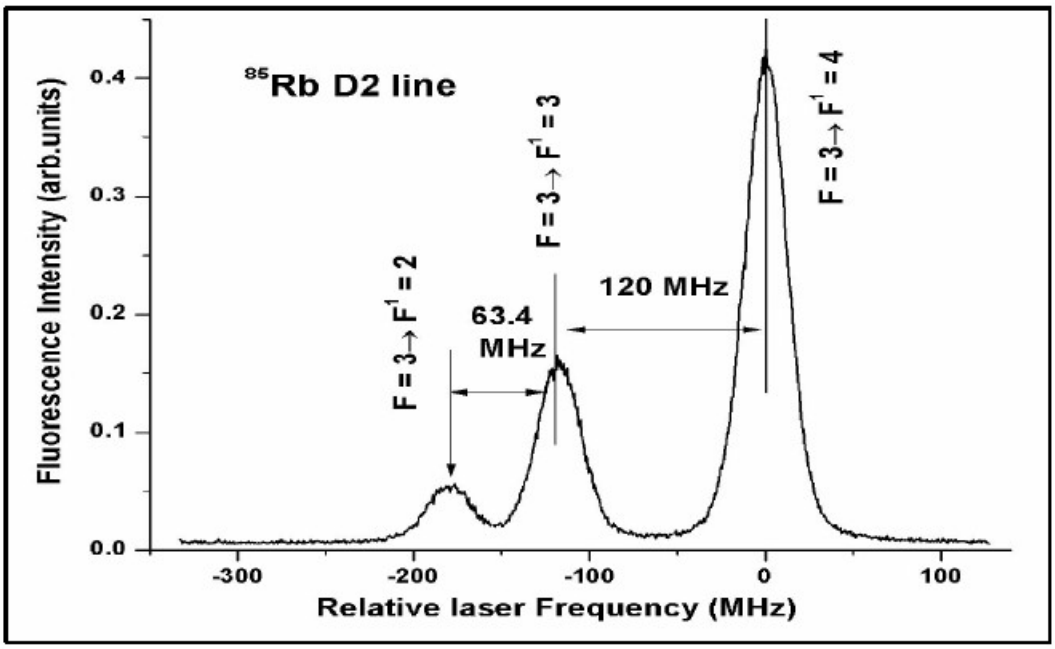

Fig.10: The sub-Doppler peaks for the ^{85}Rb isotope for the D2 transition have been recorded. The hyperfine components are F = 3 to F^1 = 2, F = 3 to F^1 = 3and the F = 3 to F^1 = 4 component respectively.

The natural width of the $5^2S_{1/2}$– $5^2P_{3/2}$ D2 line for ^{87}Rb isotope is 6 MHz.The expression for saturation intensity (I_{sat}) is

$$I_{sat} = \frac{\pi A_{21} hc}{\lambda^3} \tag{3}$$

Where, A_{21} is the Einstein's coefficient, and λ is the wavelength of the transition.The saturation intensity for this transition is 1.6 mW/cm^2 . The intensity has been varied to study the behaviour of power broadening. The width due to power broadening (Γ)is given by the expression

$$\Gamma = \Gamma_0 \sqrt{\left[\left(1 + \frac{I}{I_{sat}}\right)\right]} \tag{4}$$

The intensity used for some of the experiments is 2.7 mW/cm^2 and the width due to power broadening Γ is 9.8 MHz. The width due to transit time broadening $\delta\nu_{tt}$ is given by the expression

$$\delta\nu_{tt} = \frac{\nu_{beam}}{d} = \sqrt{\frac{\left(2kT/M\right)}{d}} \tag{5}$$

Where ν_{beam} is, the velocity of the atomic beam and are 428 m/s for a temperature of 950 K and d is the diameter of the laser beam which is 3 mm. The transit time broadening $\delta\nu_{tt}$ is ~ 0.1 MHz.The contribution from Doppler broadening has been brought down to ~ 6 MHz. Thus the FWHM of the sub-Doppler peak is an addition from all these contributions(lifetime, power, transit-time and Doppler broadeneing) adds to ~16 MHz.Atomic fluorescence from atomic potassium has also been recorded. The sub-Doppler spectra of the $4^2S_{1/2}$– $5^2P_{1/2}$ D1 transition of potassium for the ^{39}K and the ^{41}K isotope for two different frequency ranges covering different hyperfine components have been recorded. The F = 2 to F^1 =1 and the F = 2 to F^1 = 2 hyperfine component of the ^{41}K isotope appears at the start of the ramp (Fig.11). The two components have a relative intensity of 100 and 100 (arb. units) respectively and are not resolved and their separation is also ~ 30.5 MHz. The F = 1 to F^1 =1 and the F = 1 to F^1 = 2 hyperfine component of the ^{39}K isotope appears at the middle of the ramp (Fig.11).

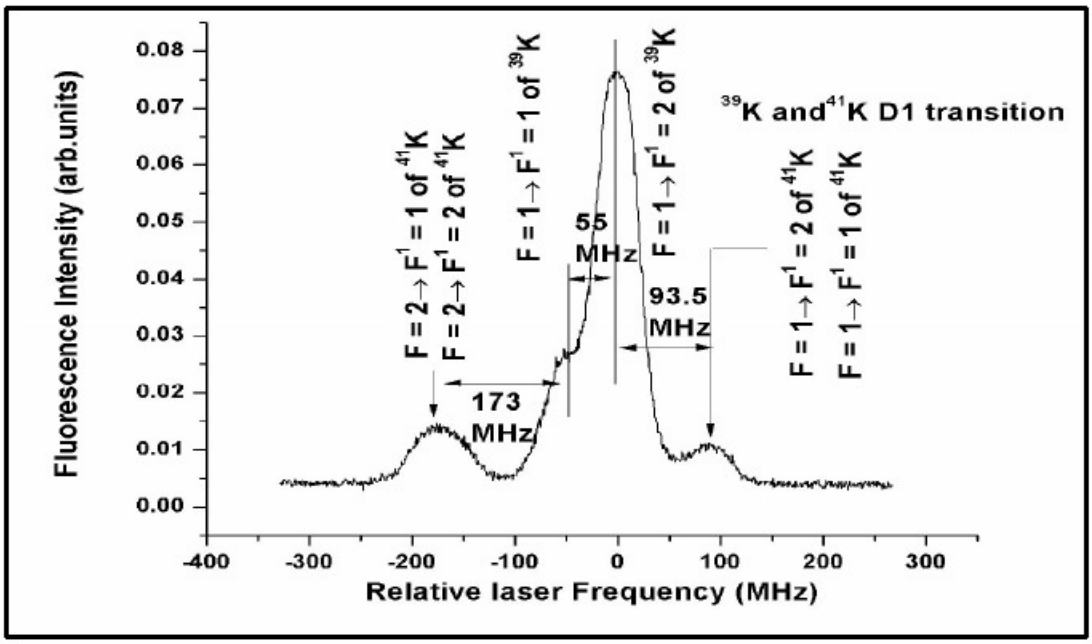

Fig.11:The F = 2 to F^1 =1 and the F = 2 to F^1 = 2 hyperfine component of the ^{41}K isotope appears as a single peak and their separation is ~ 30.5 MHz at the start of the ramp. The F = 1 to F^1 =1 and the F = 1 to F^1 = 2 hyperfine component of the ^{39}K isotope appears at the middle as a single peak with a separation of ~ 55.5MHz.The F = 1 to F^1 =1 and the F = 1 to F^1 = 2 hyperfine component of the ^{41}K isotope appears as a single peak at the end with a separation of ~ 30.5MHz.The scan range of the laser is 650 MHz and power is 23 □W

The two components have a relative intensity of 20 and 100 (arb. units) respectively and are not resolved and their separation is ~ 55.5 MHz. The F = 1 to F^1 =1 and the F = 1 to F^1 = 2 hyperfine component of the ^{41}K isotope appears at the end of the ramp. The two components have a relative intensity of 20 and 100 (arb. units) respectively and are not resolved and their separation is ~ 30.5 MHz. The total scan range of the laser is 650 MHz and the laser was scanned from 389.286050 THz to 389.286600 THz. The laser was operated at a power of 23 μW (Fig.11). The laser was then tuned to a different frequency range to cover a different set of hyperfine component of ^{39}K isotope. The F = 2 to F^1 = 1 hyperfine component of ^{39}K isotope and the F = 2 to F^1 = 2 hyperfine component of the ^{39}K isotope whose separation is ~ 55.5 MHz have also been recorded. The laser was operated at a power of 23 μW and the temperature of the atomizer was maintained at ~950K for all the experiments (Fig. 12).

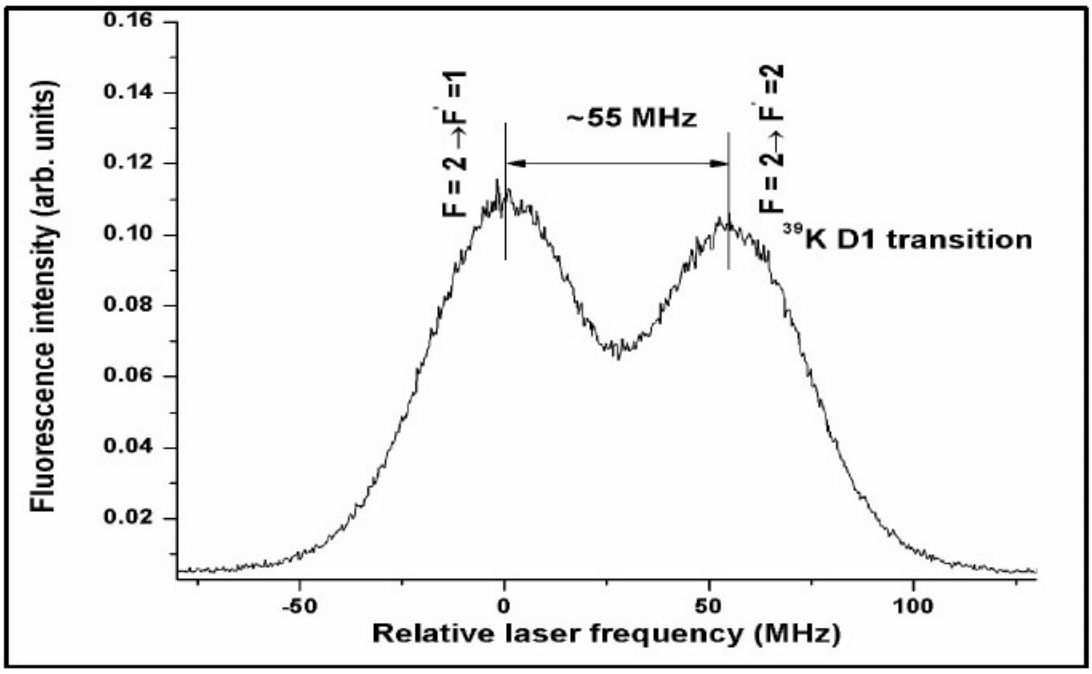

Fig. 12 The sub- Doppler peaks for the ^{39}K isotope for the $4\,^2S_{1/2}$ - $5\,^2P_{1/2}$ D1 transition have been recorded for a laser power of 23 μ W. The separation between the F= 2 to F^1 =1 and F = 2 to F^1 = 2 hyperfine component of ^{39}K isotope is 55 MHz

Number density calculations

Asdiscussed in the previous section atomic effusion from the source has been established as the pressure of the metal vapour is less than 10^{-1} mm of Hg and the aperture of the oven is 2 mm. The total number of atoms leaving the source (dN_{total}/dt) can be calculated using the expression [4]

$$\frac{dN_{total}}{dt} = \left[\frac{F \times P_K}{k_B \times T}\right] \tag{7}$$

The number density is estimated to be 2.7×10^{14} atoms/sec.

Where, F is the crucible conductance, $P_K$the partial pressure of rubidium at temperature T [19], k_B is the Boltzmann constant.Assuming anatomic flow regime,

$$F = \left[\frac{2 \times \pi \times a^3 \bar{\upsilon}}{3 \times L}\right] \tag{8}$$

Where Land a are the length and radius of the crucible and $\bar{\upsilon}$ is the most probable velocity of the rubidium atomic beam. In the present experiments,F= 3.6×10^{-5} m^3/sat T

= 960 K. The partial pressure of rubidium is 1 X 10^{-6} atmosphere at this temperature [18]. Under atomic effusion conditions the angular distribution of atoms effusing through a narrow aperture source at an angle θ into a solid angle dω is a cosine distribution. The mean free path is greater than the length of the tube and atomic effusion has been established. Under this condition, the beam is highly directional, the angular spread being given by the dimensions of the aperture, and the peak intensity (atoms/s/sr) and the flow rates N (atoms/sec) are proportional to the pressure in the source. The intensity of atoms [I (θ) d Ω] is given by the expression [3]

$$I(\theta)d\Omega = \left[\frac{n_o \times \bar{\upsilon} \times S \times Cos(\theta) \times d\Omega}{4 \times \pi}\right] \quad (9)$$

dΩ is the solid-angle subtended by the atomic beam at the interaction region. The intensity in the forward direction (θ = 0) is given by the expression

$$I(0) = \left[\frac{8.55 \times 10^{21} \times p_o \times S}{\sqrt{M \times T}}\right] \quad (10)$$

Where p_o is the pressure in mbar, M is the molecular weight (amu) and Tis the temperature in K.The intensity of atoms in the forward direction I (0) is estimated to be 1 X 10^{18}(atoms per steradian and sec).The intensity $I_{channel}$at the interaction region is given by the expression

$$I_{channel} = W I \quad (11)$$

Where W is 4d / 3L where d is the diameter and L is the length of the collimator. 3L/ 4d is known as the quality factor which is 20 for our atomizer and gives the increase in the forward beam intensity at a fixed consumption rate as compared to a thin aperture or a filament source. W is the inverse of the quality factor and is 0.05 for our system.In our particular case the L/d >> 1, the flow of atoms is transparent. The intensity of atoms $I_{channel}$at the interaction region is estimated to be 5 X 10^{16}(atoms per steradian and sec).The atom density was also rechecked by calculating the individual efficiencies of the various processes that are involved right from the release of an atom from the crucible to the detection of fluorescence from the atom. The total efficiency (η_{total}) of the process is given by the expression:

$$\eta_{total} = \eta_{release} \times \eta_{delivery} \times \eta_{irradiation} \times \eta_{selectivity} \times \eta_{detection} \quad (12)$$

The $\eta_{release}$ is calculated to be 25 x 10^{-2}, $\eta_{delivery}$ is 6 x 10^{-2}, $\eta_{irradiation}$ is 7 x 10^{-4}, $\eta_{detection}$ is determined to be 1.6 x 10^{-5}.The selectivity of fluorescence detection $\eta_{selectivity}$ is 0.125. The detection efficiency $\eta_{detection}$ is the product of the efficiency of the PMT (η_{PMT}) and the solid angle of detection (Ω)

$$\eta_{detection} = \Omega \times \eta_{PMT} = 0.005 \times 3.2 \times 10^{-3} = 1.6 \times 10^{-5} \quad (13)$$

Thus the overall efficiency η_{total} is 2.1 x 10^{-11}. The atom density in the crucible is 7 x 10^{20} atoms of rubidium.The crucible has been operated for a period of 120 hours. The calculation of the number of atoms /sec has been rechecked by dividing the amount of rubidium atoms present in the crucible and the hours of operation of the crucible. The number density is ~ 3 X 10^{14} atoms/sec as calculated using eq.7.

Conclusions

We have demonstrated a simple yet versatile atomic beam apparatus for atomic beam fluorescence experiments. We have studied the evolution of the system from Doppler broadened conditions to Doppler limited conditions which enabled us to study the sub-Doppler hyperfine spectroscopy of rubidium and potassium. We have recorded the sub-Doppler spectrum of ^{85}Rb and ^{87}Rb isotopes and the FWHM of the peaks recorded is ~16 MHz for the $5^2S_{1/2} - 5^2P_{3/2}$D2 transition of rubidium close to the natural broadening of this transition. We have also recorded the sub-Doppler spectrum of ^{39}K and ^{41}K isotopes for different frequency ranges for the $4^2S_{1/2} - 5^2P_{1/2}$ D1 transition of potassium in order to record the different hyperfine components. The small thermal mass of the source makes the turn-on and the turn – off time relatively less in comparison to the hours of operation of the atomic beam. The turnaround time is about 2 hours. The compact interaction geometry, flexibility in changing the atomic beam source and simplicity of the entire set up makeit useful for the measurement of isotope shifts and hyperfine structure measurement of single / multistep excitations of various elements.

Reference

1. Timothy M. Roach and Dwayne Henclewoode.(2004). Novel rubidium atomic beam with an alkali dispenser source, *J. Vac. Sci. Technol. A* 22(6), 2384-2387.
2. Umakant D. Rapol, Ajay Wasan, and VasantNatarajan.(2001) Loading of Rb from a magneto optic trap from a getter source,*Phys. Rev. A**64*, 023402 [5pages].
3. Norman F. Ramsey. (1956). *Molecular Beams*,Oxford University Press, Oxford.
4. Yoshihiro Iwata, Yoshizumi Inoue, Makoto Minowa(2009) Trace element analysis of potassium by resonance ionization mass spectrometry,*Jpn. J. Appl. Phys. 48*, 076505 [2 pages].
5. S. Aubin, E. Gomez, L. A. Orozco, and G. D. Sprouse, (2003) High efficiency magneto optical trap for unstable isotopes,Rev. Sci. Instrum. 74 (10), 4342 -4351.
6. A. Sargsyan, D. Sarkisyan, and A. Papoyan.(2006). Dark-line atomic resonances in a submicron-thin Rbvapour layer.*Phys. Rev. A 73,* 033803 [7 pages].
7. E. Gomez, F. Baumer, A. D. Lange, and G. D. Sprouse and L. A. Orozco. (2005).Lifetime measurement of the 6s level of rubidium,*Phys. Rev. A 72*, 012502[9 pages].
8. A. Pérez Galván, Y. Zhao, and L. A. Orozco.(2008).Measurement of the hyperfine splitting of the $6s_{1/2}$ level in rubidium.*Phys. Rev. A 78,* 012502 [11 pages].
9. J.C. Camparo, S.B. Delcamp. (1995)Optical pumping with laser induced fluorescence, Optics Communications 120, 257 –263.
10. I.M. Beterov *, V.M. Entin, I.I. Ryabtsev, Spectrochim.Acta A 55 (1999) 2111 - 2119.
11. A. Hernández-Hernández, E. Méndez-Martínez, A. Reyes-Reyes, J. Flores-Mijangos, J. Jiménez-Mier, M. López, E. de Carlos. (2009)*Optics Communications* 282,887 -891.
12. Altaf H. Nizamani, James J. McLoughlin and Winfried K. Hensiger. (2010).*Phys. Rev. A 82*, 043408 [6 pages].
13. Sven Mannervick. (2000).Hyperfine Interactions, 127,237 -245.
14. V.Gerginov and Carol.E. Tanner. (2003).Optics Commun. 222, 17 – 28.
15. J. E. Lawler, G. Bonvalletand C. Sneden.(2001). Experimental radiative lifetimes, branching fractions, and oscillator strengths for La II and a new determination of the solar lanthanum adundance, The Astro. Phys. Journal,556,452 -460.

16. L. Ebdon, E. Hywel Evans. (1998).An introduction to analytical atomic spectrometry, John Wiley & Sons Inc., NewYork.
17. Christopher J. Foot. (2005).*Atomic Physics,* Oxford University Press, Oxford.
18. C.E. Adams, M.H. Rowell, and J.T.Quan. (1970).*High temperature measurements of the rate of uptake of rubidium chloride vapour by selected oxides*.NOLTR 69 -191, Naval Ordnance Laboratory, White Oak, Silver Spring, Maryland.

INTERNATIONAL JOURNAL OF INNOVATIVE RESEARCH & DEVELOPMENT

ISSN: 2278 – 0211 (Online) / 2278-7631 (Print)

A Study On Data Backup And Recovery Procedure At A Cooperate Hospital

Syed Murtuza Hussain Bakshi
Vice Principal and Associate Professor
Department of hospital management,
Owaisi Hospital and Research Center,
Hyderabad,India

Shaista amreen
OT Manager
Owaisi Hospital and Research Center,
Hyderabad, India

Abstract:

Computer users all across the world are familiar with the problem of lost data such incidents may result in lost work or the deletion of unnecessary files or even loss of important business data that has significance and cost associated with it. Information is an asset like other important business assets which is essential to an organization and consequently needs to be suitably protected especially in interconnected business environment where information is exposed to a growing number and a wider variety of intimidation and vulnerabilities. Management should provide a means to backup relevant data on a regular basis. There are key backup issues that have to be concerned by the management they are media of backup, the reliability of backup process, where the backup is stored and testing the procedure for restoring the backup at least once a year. The study was conducted at 14 tertiary care hospitals with an aim to study various hospital information systems, regular data backup and recovery practices & procedures, comprehend the hardware and network layout. Data is analyzed through Logical and Metaphorical Analysis. It was found out in the study that the backup methods that are followed at the tertiary care hospitals are Incremental Backup and Full Backup with a standard hardware support.

Keywords: *Computers, Data backup and recovery, Hospital Information Systems.*